

A novel dual-plasmid platform provides scalable transfection yielding improved productivity and packaging across multiple AAV serotypes and genomes

Laura P. van Lieshout,¹ Miranda Rubin,² Katrina Costa-Grant,¹ Stacy Ota,¹ Diane Golebiowski,¹ Troy Panico,¹ Eli Wiberg,¹ Klaudia Szymczak,¹ Richard Gilmore,¹ Marissa Stanvick,¹ Brenda Burnham,¹ Jeff Gagnon,¹ Ifeyinwa Iwuchukwu,¹ Guang Yang,¹ Iraj Ghazi,¹ Alex Meola,¹ Ryan Dickerson,¹ Thomas Thiers,¹ Luke Mustich,¹ April Hayes,² Israel Rivas,² Jason Lotterhand,² Nancy Avila,² James McGivney,¹ Jin Yin,¹ and Tim Kelly¹

¹Oxford Biomedica Solutions LLC, 1 Patriots Park, Bedford, MA 01730, USA; ²Homology Medicines, Inc., 1 Patriots Park, Bedford, MA 01730, USA

Transient transfection of mammalian cells using plasmid DNA is a standard method to produce adeno-associated virus (AAV) vectors allowing for flexible and scalable manufacture. Typically, three plasmids are used to encode the necessary components to facilitate vector production; however, a dual-plasmid system, termed pDG, was introduced over 2 decades ago demonstrating two components could be combined resulting in comparable productivity to triple transfection. We have developed a novel dual-plasmid system, pOXB, with an alternative arrangement of sequences that results in significantly increased AAV vector productivity and percentage of full capsids packaged in comparison to the pDG dual design and triple transfection. Here, we demonstrate the reproducibility of these findings across seven recombinant AAV genomes and multiple capsid serotypes as well as the scalability of the pOXB dual-plasmid transfection at 50-L bioreactor scale. Purified drug substance showed a consistent product quality profile in line with triple-transfected vectors, except for a substantial improvement in intact genomes packaged using the pOXB dual-transfection system. Furthermore, pOXB dual- and triple-transfection-based vectors performed consistently *in vivo*. The pOXB dual plasmid represents an innovation in AAV manufacturing resulting in significant process gains while maintaining the flexibility of a transient transfection platform.

INTRODUCTION

Transient transfection of human embryonic kidney (HEK) 293 cells is a common manufacturing strategy for adeno-associated virus (AAV) vectors for both academic and industry applications. Transfection-based systems offer the advantage of being quicker and more flexible than baculovirus/herpes simplex virus infection-based systems or producer cell lines that require significantly more up-front development compared with plasmid generation. Historically, recombinant AAV (rAAV) production relied on infection of cells with a replication competent helper virus to provide a cellular environment conducive

to AAV replication and gene expression. However, due to initial safety concerns regarding adenovirus contamination in purified AAV products, helper virus infection has largely been replaced with transfection of a helper plasmid containing the required genes for AAV production but cannot facilitate helper virus generation.¹ Traditionally, three plasmids are supplied for triple transfection that each deliver the required genetic components to produce rAAV: (1) an AAV genome plasmid containing the gene of interest (GOI) expression cassette with appropriate regulatory elements flanked by inverted terminal repeats (ITRs), (2) a RepCap plasmid that provides the AAV replicase and capsid gene expression *in trans*, and (3) a helper plasmid providing helper virus functions as described above.² Currently, Luxturna and Zolgensma are the only US Food and Drug Administration (FDA)-approved AAV gene therapies on the market and are both manufactured by transient transfection, highlighting the safety and utility of transfection-based AAV production for current good manufacturing practices (cGMP) use.^{3,4}

Transient transfection approaches are not limited to triple transfection. In the late 1990s, Dirk Grimm and colleagues demonstrated the feasibility of a dual-plasmid transfection approach for AAV production.⁵ The pDG dual system combines the RepCap and adenovirus helper plasmids into a single plasmid to be transfected along with a separate GOI-ITR-flanked construct. A dual-plasmid transfection offers the obvious advantage of fewer plasmids to manufacture and manage, while also streamlining the transfection unit operation. A recent study evaluated a pDG-inspired dual design with modifications to the backbone to meet cGMP requirements and facilitate generation of multiple capsid serotype versions of the construct.⁶ This version of

Received 1 September 2022; accepted 4 May 2023;
<https://doi.org/10.1016/j.omtm.2023.05.004>.

Correspondence: Laura P van Lieshout, Oxford Biomedica Solutions LLC, 1 Patriots Park, Bedford, MA 01730, USA.

E-mail: l.vanlieshout@oxb.com

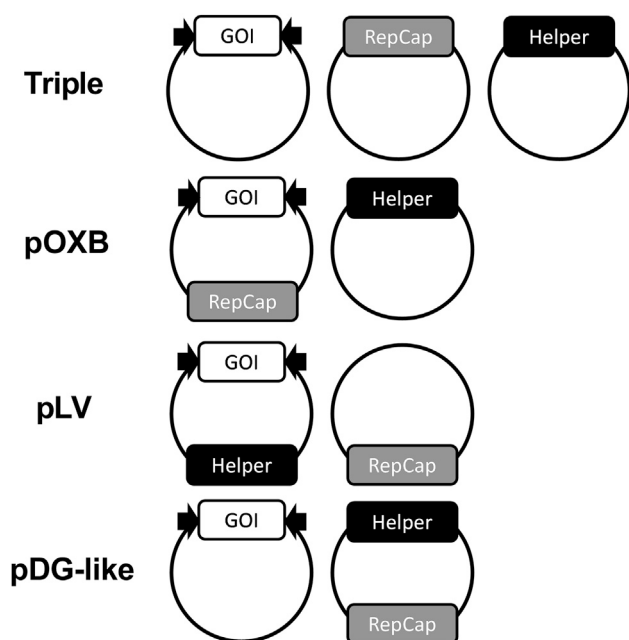


Figure 1. Schematics of dual- and triple-plasmid design configurations

RepCap+helper plasmid, termed pQT, was compared with triple transfection for AAV1, AAV5, AAV8, and AAV9 capsids, which resulted in comparable productivity for both transfection platforms.⁶

We sought to evaluate a dual-plasmid system as an alternative to triple transfection for manufacturing AAVs derived from human hematopoietic stem cell (AAVHSC) gene therapy and gene editing vectors. AAVHSCs are a class of AAV clade F capsids isolated from human CD34+ peripheral blood stem cells that demonstrate transduction profiles in a variety of disease-relevant tissues in non-human primates, and AAVHSC15 is currently being evaluated in the clinic (NCT03952156).^{7,8} In addition to reducing the number of plasmids required, we also aimed to increase vector genome (VG) productivity and improve product quality using the same triple-plasmid components already a part of our process.

RESULTS

pOXB dual-plasmid design outperforms pDG-like, pLV dual plasmids and triple-plasmid productivity

To investigate the potential of a dual-plasmid transfection for rAAV production, we sought to evaluate different dual-plasmid configurations beyond the historical pDG system.^{5,9} There are three possible configurations of the components of triple transfection into dual plasmids (Figure 1). Identical RepCap, helper, and AAV genome sequences were used to generate the plasmids for all experiments described here. As such, we have denoted the RepCap+helper design, pDG-like, as it is inspired by the original pDG design but does not contain the MMTV promoter for Rep expression since our goal was to maintain identical sequences from triple transfection to a new dual design.

The pOXB dual plasmid combines the GOI-ITR+RepCap sequences together on a single plasmid and provides helper functions separately, while a second dual-plasmid design, termed pLV, combines GOI-ITR+helper sequences together and provides the RepCap plasmid separately (Figure 1). To the best of our knowledge, pOXB and pLV constitute novel dual-plasmid configurations. The pOXB, pDG-like, and pLV dual plasmids were all compared with triple transfection in a shake flask model using suspension HEK293 cells at a 1:1 or 1:1:1 M ratio respectively. Equal molar ratios were selected for initial screening as the fairest way to assess two- and three-plasmid systems that contain various sized molecules (Table S1).

In terms of VG productivity, the pOXB dual significantly outperformed pLV by 2.2x, triple by 2.5x, and pDG-like by 2.9x (Figure 2A). Capsid productivity for the pLV and pDG-like dual systems were proportionally higher than the produced VGs, resulting in the lowest calculated full vectors of the tested designs (Figures 2B and 2C). Triple transfection resulted in 15% full vectors, while vectors generated by the pOXB dual system were 20% full (Figures 2B and 2C). Expression of Rep proteins is relatively similar among all tested conditions; however total capsid expression is notably stronger for all the dual-plasmid systems compared with triple transfection, which is also reflected by the capsid ELISA titers (Figures 2D–2G). However, there were no remarkable differences in Rep or Cap expression between dual-plasmid designs that point to mechanism of increased productivity in pOXB duals.

While equal molar ratios were a fair starting point for comparing triple and various dual-plasmid systems, it is unclear if it is the most optimal ratio for each transfection. A shake flask study comparing six various molar ratios for triple transfection was completed to determine the best condition for comparison to dual-plasmid systems. A ratio of 1:2:1 GOI-ITR:RepCap:helper produced the highest VGs and was an increase of 27% over the 1:1:1 equal molar ratio (Figure S1).

Previous studies optimizing pDG dual-plasmid transfection conditions typically utilized equimolar ratios.⁶ However, a recent study optimizing pQT, another pDG adjacent dual plasmid, found molar ratios of 2:1 or 1:1 GOI-ITR:RepCap+helper resulted in the highest VG yields.⁸ Using these previous publications as a foundation, we sought to further optimize the dual-plasmid systems by evaluating molar ratios of 2:1, 1:1, and 1:3.

While equal molar ratios were not optimal for all systems, changing the ratios did not make a drastic difference in their performance (Figure 3). pOXB was superior to pLV and pDG-like duals as well as triple transfection at the best performing ratios respectively. Again, no notable trends were observed in the western blot analysis of Rep and Cap expression utilizing different plasmid ratios (Figure S2).

In an effort to understand if the MMTV promoter replacing the native p5 is critical to the success of the original pDG dual-plasmid design, the pDG-like Rep promoter was altered to align with the MMTV-Rep

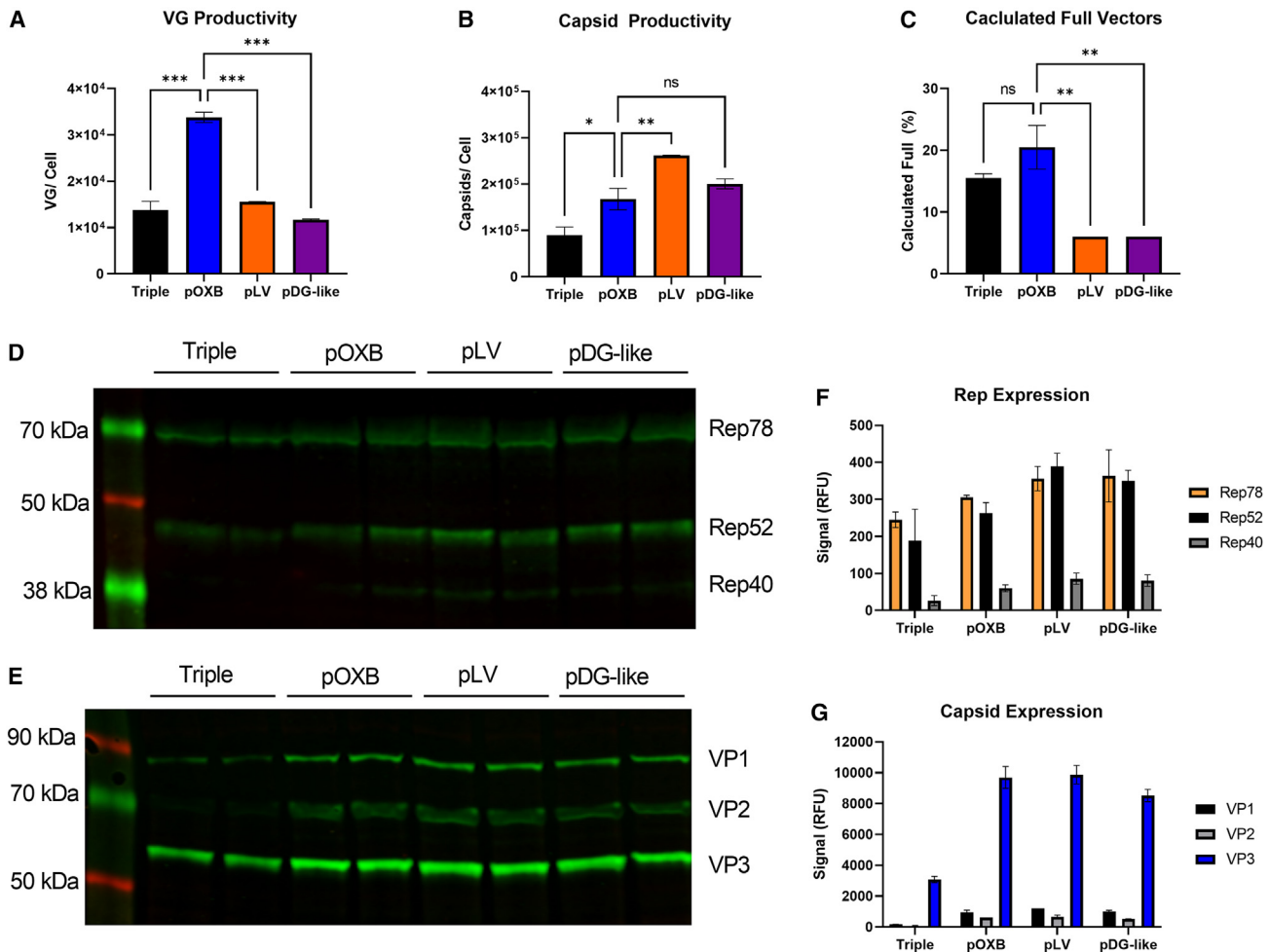


Figure 2. Productivity assessment of three possible dual-plasmid configurations and triple transfection

Shake flasks were transfected with pOXB, pLV, or pDG-like dual or triple plasmids using GOI-ITR genome G sequence at a 1:1 or 1:1:1 M ratio. Crude lysate samples were quantified for (A) VG productivity, (B) capsid productivity, and (C) the percentage of calculated full vectors. Western blot analysis was performed on crude lysates to detect (D) Rep and (E) Cap expression. Quantification of (F) Rep and (G) Cap expression from the western blot is shown. All conditions were completed in duplicate, and the data are displayed as mean \pm SD. Statistical significance was calculated using a one-way ANOVA, * $p < 0.05$, ** $p < 0.01$, *** $p < 0.001$.

sequence from pDG. This new version pDG-like-MMTV did not improve the performance of the RepCap+helper configuration, as VG productivity was the same or less than pDG-like with intact p5-Rep (Figure S3). Rep78 expression was reduced in crude lysates transfected with pDG-like-MMTV compared with pDG-like with native p5, which is consistent with previous literature; however, in our process, this altered Rep expression did not have a desired effect.⁵ In order to benchmark these results against the original pDG, we purchased the AAV9 version from Plasmid Factory (pDP9) and included it in the comparison of the pDG-like versions. The pDP9 VG productivity was consistent with the other pDG-like designs; however capsid expression was substantially higher (Figure S3).

pOXB dual transfection generates the highest calculated full vectors in the crude lysate. It is well known that helper genes promote the acti-

vation of Rep and Cap promoters.¹⁰ Therefore, since pDG-like links the helper and RepCap sequences on a single plasmid, perhaps this generates excess capsid background and points toward the mechanism of pOXB dual improvements in full vectors. In an effort to understand this further, capsid titers were quantified following transfection of the complete pDG-like and pOXB dual systems alongside transfections of only the RepCap-bearing plasmid to determine background capsid expression in each system. The pDG-like RepCap+helper plasmid alone produced 70% as much capsid as the complete pDG-like dual transfection, while the pOXB ITR-GOI+RepCap plasmid only generated 0.2% as many capsids as the complete pOXB dual system (Figure S4). However, like the pOXB design, the pLV dual system does not link RepCap and helper, so this alone cannot explain the mechanism for pOXB improvements. We speculate the pOXB design may produce an ideal stoichiometry

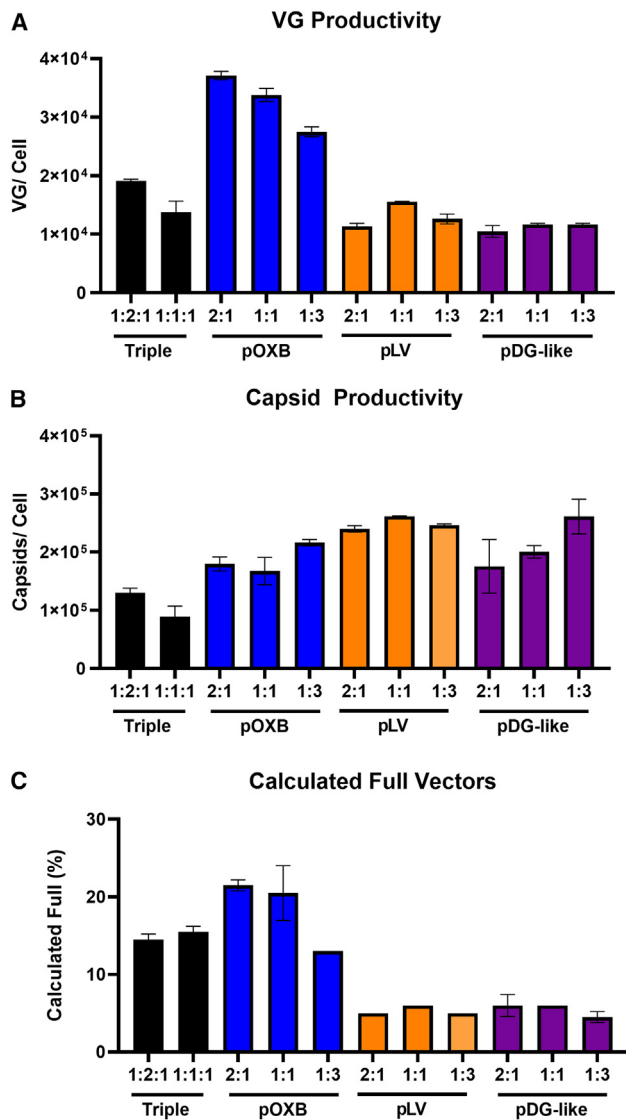


Figure 3. Productivity assessment of pOXB, pLV, and pDG-like dual plasmids compared with triple transfection

Shake flasks were transfected with pOXB, pLV, or pDG-like dual plasmids at molar ratios of 2:1, 1:1, and 1:3 with the first plasmid containing the GOI-ITR sequence. Triple transfection is shown at a 1:2:1 and 1:1:1 M ratio GOI-ITR:RepCap:helper. Crude lysate samples were quantified for (A) VG production, (B) capsid production, and (C) calculated full vectors. All conditions were completed in duplicate, and the data are displayed as mean \pm SD.

among the GOI-ITR, RepCap, and helper sequences compared with the other dual systems. This hypothesis is supported by the fact that ITRs and RepCap exist as *cis* elements in wild-type AAV, and others have noted the concept of *cis*-packaging being more efficient and producing fewer empty capsids than when RepCap is supplied *in trans*.^{11,12} However, the exact mechanism of the pOXB dual improved VG productivity and packaging is still left to be fully understood.

The differences in dual design productivity demonstrate that the components required for AAV production can be delivered in an optimal manner through a mechanism other than simply reducing the number of plasmids involved in transfection. The plasmids in each transfection system vary in size (Table S1). To understand if plasmid size could be playing a role in productivity through transfection efficiency, we evaluated the number of GFP+ cells following transfection with a GFP GOI -ITR plasmid in each system. The GFP+ cells ranged from 53% to 65%, and there is no obvious trend based on plasmid size (Figure S5). The pOXB plasmid is almost double the size of the triple-GOI-ITR plasmid, but they both result in approximately 60% GFP+ cells; therefore transfection efficiency alone does not seem to explain the differences in VG productivity between plasmid designs. Overall, the pOXB dual-plasmid system outperformed the pDG-like, pDG-like-MMTV, and pLV dual plasmids as well as triple transfection in terms of VG productivity and calculated percentage of full vectors in crude lysate. Therefore, we moved forward with further characterization of this novel pOXB dual-plasmid system.

pOXB dual-plasmid system results in improved productivity and vector quality across multiple vector constructs

Following the promising preliminary observations with the pOXB dual-plasmid system, we evaluated a total of seven different rAAV genomes ranging from ~2,200 to 4,600 nucleotides in length and containing multiple different promoters and transgenes in 2-L bioreactors (Table S2). Compared with triple transfection, there was an increase in VG productivity between 34% and 222% and an increase of calculated percent full vectors between 24% and 214% across all seven genome constructs (Figures 4A–4C). Genomes A–E and G were packaged with AAVHSC15, and genome F was packaged with AAVHSC17, demonstrating the pOXB dual-plasmid system is compatible with multiple AAVHSC capsids. Furthermore, the AAV2 capsid sequence was incorporated into the pOXB dual system to establish the feasibility of this plasmid design across more diverse, non-clade F serotypes. The AAV2 pOXB dual transfection outperformed triple transfection productivity by over 3-fold and demonstrated similar improvements in full vectors as seen for the AAVHSC capsids (Figure 5). AAV2 is the prototypical AAV capsid, and these data highlight the novel pOXB dual-plasmid approach to improve productivity and full capsid production for serotypes beyond the AAVHSC panel. Overall, these data demonstrate the pOXB dual design is functional across multiple rAAVs, including single-stranded and self-complimentary genomes, four distinct transgenes and promoters, as well as two diverse capsid clades.

In addition to higher productivity compared with triple transfection, the pOXB dual system also generates improved packaging profiles by increasing the proportion of full-length intact rAAV genomes in purified AAV lots. A number of accepted analytical methods can be used to determine the packaging profile of rAAV capsids, including the charge detection mass spectrometry and transmission electron microscopy, using the ratio of VG titer compared with the capsid titer and analytical ultracentrifugation (AUC).¹³ Following the upstream

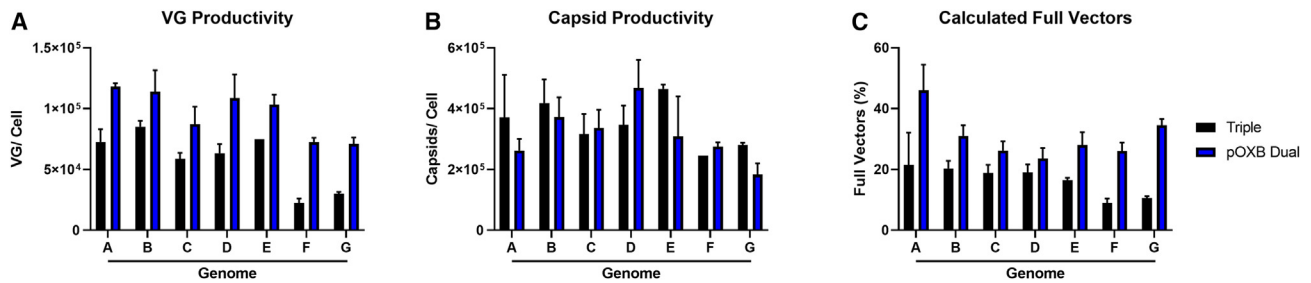


Figure 4. Productivity assessment of seven AAV genomes comparing pOXB dual to triple transfection

Transfections were performed with pOXB dual or triple plasmids for each GOI-ITR genome sequence in 2-L bioreactors. Crude lysate samples were quantified for (A) VG production, (B) capsid production, and (C) calculated full vectors. All vectors were packaged with AAVHSC15 except for genome F, which was packaged with AAVHSC17. All conditions were completed at a minimum of $n = 2$, and the data are displayed as mean \pm SD.

process in bioreactors, vectors in crude lysate were subjected to affinity chromatography and anion exchange chromatography prior to formulation. Samples of purified vector were analyzed by AUC to determine the proportion of capsids containing full-length intact genomes, partial genomes, or empty capsids. Vectors produced with pOXB dual transfection demonstrated improvements in intact genomes packaged compared with triple transfection. Intact genomes increased by 14%, 7%, 15%, and 29% for genomes B, C, D, and F, respectively (Figure 6A). Furthermore, the pOXB dual-plasmid system resulted in reductions of up to 17% of partial packaged genomes (Figure 6B) and a decrease of up to 13% in the number of empty capsids present in the purified vector compared with triple transfection across four distinct rAAV genome designs (Figure 6C). Reductions in these partial genomes and empty capsids in combination with the increase in full intact genomes packaged represent significant improvements in the vector product quality profile, which is key to providing safe and effective therapies for patients.

Increased productivity with pOXB dual system scales to 50-L bioreactors, and extended product quality panel remains consistent with triple transfection

Next, the pOXB dual-plasmid transfection was scaled up to a 50-L bioreactor to ensure this process yielded similar results at a larger scale more representative of cGMP manufacturing. Our transfection-based rAAV manufacturing platform has demonstrated linear scalability from 50-L to 500-L and to 2000-L bioreactors; therefore, the 50-L scale is utilized to confirm process changes as a representative large-scale model (Figure S6). Consistent with the trends at 2-L bioreactor scale, the results from the 50-L bioreactors demonstrated an almost 2-fold increase with genome D in VG productivity, comparable capsid production, and a doubling in the calculated full vectors in the crude lysate (Figures 7A–7C). These data support the pOXB dual-plasmid system as a scalable process, which yields consistent results across all tested production scales.

When introducing process changes, it is crucial that the vector quality profile remains consistent or improved compared with historical data. We evaluated purified vectors produced using pOXB dual or triple transfection with an extended panel of analytics to characterize prod-

uct quality. The overall downstream VG recoveries between pOXB dual plasmids and triple transfection were highly similar, specifically within a 4% difference. Purity, aggregation, and residual host cell protein all remained consistent regardless of transfection method, which is expected as these parameters should not be impacted by plasmid-based upstream changes (Figures 7D–7F). Furthermore, there were no significant differences in residual host cell DNA, RepCap, E1A, or helper sequences packaged in the pOXB dual vectors (Figures 7G–7I). It is worth highlighting that despite the RepCap and GOI-ITR sequences being located on the same pOXB plasmid, there was no increase in RepCap packaging compared with triple transfection, indicating the risk of recombination to generate replication competent AAV (rcAAV) is minimal despite their proximity in this plasmid design. Furthermore, an *in vitro* assay to detect rcAAV performed by an external contract research organization demonstrated rcAAV was below the limit of detection (<20 IU) for both pOXB dual- and triple-based vectors (data not shown). Overall, the pOXB dual system demonstrates an improved product quality profile in terms of packaged intact genomes (Figure 6) and remains consistent with triple transfection across an extended panel of vector analytics (Figure 7).

Triple- and pOXB dual-transfection vectors demonstrate comparable bioactivity *in vivo*

The pOXB dual-plasmid system offers increased vector yields and consistent or improved vector quality attributes compared with triple transfection; however, a direct *in vivo* comparison of vector efficacy was the final evaluation required to ensure product comparability. An rAAV genome containing a codon optimized phenylalanine hydroxylase (PAH) cDNA under the control of a liver-specific promoter was manufactured using either triple or pOXB dual transfection and injected systemically into Pah^{enu2} mice, a model displaying several features of classical phenylketonuria (PKU).¹⁴ Two doses were evaluated as well as a vehicle-only control group. Weekly serum samples were analyzed for phenylalanine (Phe) to examine the vector bioactivity as exhibited by a decrease in serum Phe concentrations. Vectors produced by triple or pOXB dual transfection were indistinguishable across both doses and throughout the 6-week observation period, demonstrating vector comparability regardless of transfection system

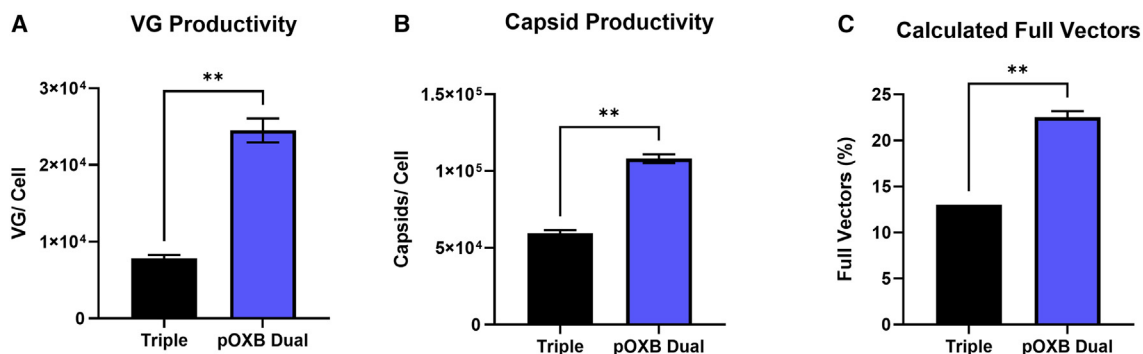


Figure 5. Productivity assessment of AAV2 with pOXB dual and triple transfection

Shake flasks were transfected with pOXB dual or triple plasmids at a molar ratio of 1:1 or 1:1:1 using the GOI-ITR genome A sequence and AAV2 capsid sequence. Crude lysate samples were quantified for (A) VG production, (B) capsid production, and (C) calculated full vectors. All conditions were completed in duplicate, and the data are displayed as the mean \pm SD. Statistical significance was determined using a Student's *t* test, ***p* < 0.01.

used for manufacture (Figures 8A and 8B). This outcome indicates that while there are productivity and product quality benefits to using the pOXB dual-plasmid system for production, the resulting vector is equivalent in potency, which is desired when changing platforms during development. Furthermore, liver VGs and *PAH* mRNA expression were quantified at endpoint, which showed a dose-dependent increase in VG transduction and transgene expression but no significant differences between the triple and pOXB dual groups at each dose (Figures 8C and 8D).

DISCUSSION

We are continuously in search of process improvements that result in more productive yields and improved vector quality, which will bring safer products to patients in an efficient and cost-effective manner. The pOXB dual-plasmid development described here demonstrates a rather simple alteration to plasmid design without introducing new sequences or heavily engineering the traditional components of triple transfection. The benefit of this type of plasmid-based improvement is that there is little impact to the rest of our platform manufacturing process or need for additional development to analytical release or characterization assays. While we are not the first to envision a dual-plasmid transfection for AAV production, to the best of our knowledge, this is the first report to investigate sequence configurations, other than the classic pDG RepCap+helper design, which also demonstrates improved performance with a dual-plasmid system.

A transfection-based AAV manufacturing platform offers multiple benefits over producer cell lines and virus infection-based approaches.¹⁵ The primary benefits are speed and flexibility. Plasmid-based changes can be introduced immediately into a transfection platform, while changes to virus stocks or producer cell lines are more laborious and time consuming to alter. As a result, non-transfection-based manufacturing platforms often require an earlier process lock, impeding new process developments from being incorporated as they become available. Additionally, it has become a common

strategy to use transfection-based AAV production for preclinical and phase I clinical trials as it is quicker and more flexible than other platforms with the intention to switch to a more “scalable” process for phase II/III or commercial supply. This approach deprives one of the depth of knowledge that is amassed from previous learnings from using the same process across all phases of product development. Furthermore, changing manufacturing platforms often involves new or different manufacturing capacities, technical process transfers, and the need for significant comparability work, all of which potentially come with a set of challenges not experienced when utilizing the same process from research grade through commercial supply of cGMP vector manufacture. Transient transfection-based AAV manufacturing is sometimes questioned as a viable approach for commercial supply; however our platform has resulted in consistent VG productivity across scale up at 50-L, 500-L, and 2000-L scale (Figure S6). The consistency demonstrated in up to 2000-L bioreactors provides evidence that transfection is in fact a viable approach for commercial supply and will allow for expansion into indications with larger patient populations. Therefore, spending resources on plasmid-based developments for improving productivity and product quality is a practical investment as outcomes like the pOXB dual-plasmid system can be incorporated into all stages of vector development in the manufacturing process resulting in continuity throughout the product life cycle.

Plasmids represent one of the most expensive raw materials of a transfection-based AAV manufacturing platform; therefore there is a clear advantage to a two-plasmid system in reduced cost of goods to produce two plasmids rather than three. While all dual-plasmid designs offer this benefit, only the pOXB dual-plasmid design provides the additional advantage of improved productivity and vector quality. The pOXB dual transfection resulted in as much as a 222% increase in productivity across seven unique genomes when compared with triple transfection under identical process conditions. In combination with other process improvements, the pOXB dual system has enabled bioreactor crude lysate titers $>1 \times 10^{15}$ VG/L.¹⁶ The pOXB

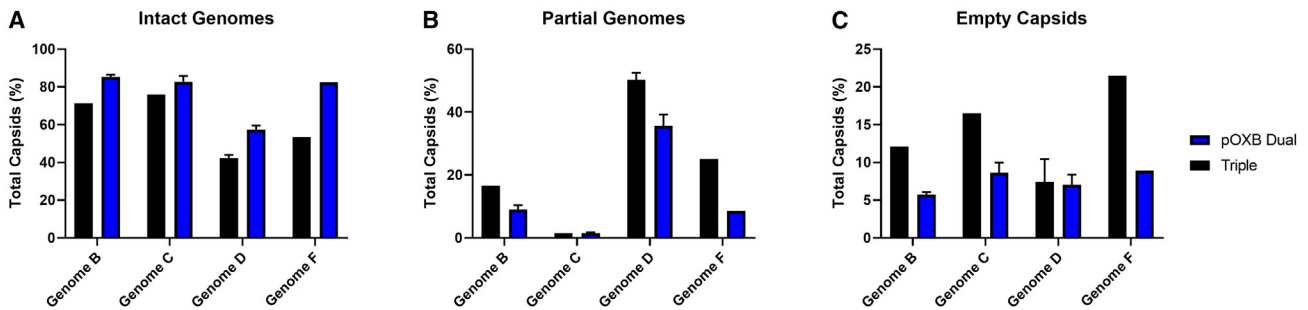


Figure 6. Increase in packaged intact vector genomes and reduction in partial packaged vectors and empty capsids observed for pOXB dual compared with triple transfection

AUC was used to analyze purified vectors produced with pOXB dual- and triple-plasmid transfection to determine the proportion of capsids containing full-length intact genomes, partial packaged genomes, or empty capsids. All data were generated at the 2-L bioreactor scale except for genome D, which was produced in 50-L bioreactors. Data are displayed as the mean \pm SD of (A) intact packaged genomes, (B) partial packaged genomes, and (C) empty capsids for pOXB dual and triple produced vectors for each genome. pOXB dual produced vectors were analyzed in the following replicates: genome B (n = 3), genome C (n = 3), genome D (n = 2), and genome F (n = 1). Triple produced vectors are all singlicate runs except genome D (n = 3).

dual-plasmid transfection also generated a higher proportion of full vectors directly out of the bioreactor than any other dual or triple transfection. This bioreactor increase is also translated downstream, resulting in fewer empty capsids present in the final vector formulation. Furthermore, the quality of the packaged genomes improved using pOXB dual plasmids, through increased full-length intact genomes packaged and reduced partial genomes packaged, which are the result of incomplete packaging or VG replication and may not be functional.^{17,18} The importance of this product quality improvement is underscored by previous clinical holds placed on AAV trials, in which high capsid loads are thought to have triggered adverse events due to elevated empty capsid content.¹⁹ Having a higher proportion of intact packaged VGs to empty capsids results in less burden to remove empty capsids downstream, providing a safer product for patients. The importance of a high-quality packaging profile is underscored by the FDA discussions on the topic at the Gene Therapies Advisory Committee Meeting in 2021.²⁰ As AAV gene therapy is a rapidly evolving field, guidance for CMC requirements is becoming more informed, and it is critical that process development with the goal of improving packaging profiles and reducing impurities and process residuals is prioritized as product quality becomes the cornerstone of successful AAV vector manufacturing.

MATERIALS AND METHODS

Plasmids

All plasmids were generated using In-fusion cloning (TakaraBio, San Jose, CA) and scaled up at Aldevron (Fargo, ND). pOXB plasmids were cloned by inserting the RepCap cassette into the backbone of the GOI-ITR plasmid, pDG-like plasmids were cloned by inserting the RepCap cassette into the backbone of the helper plasmid, and pLV plasmids were cloned by inserting the helper genes into the backbone of the GOI-ITR plasmid. ITR-bearing plasmids were subjected to Sanger sequencing and restriction enzyme analysis using SmaI and AhdI to confirm the ITRs were intact. The GOI-ITR, RepCap, helper, and backbone sequences in all plasmids are identical, regard-

less of configuration as a triple transfection system or any of the dual combinations with the exception of pDP9, which was purchased directly from Plasmid Factory (Bielefeld, Germany). All plasmids utilized the HSC15 capsid sequence unless otherwise noted in the figure legend.⁷

Productivity assessment

Expi293F cells (Thermo Fisher, Waltham, MA) were expanded for at least one passage and inoculated into a shake flask or single-use bioreactor containing Expi293 cell culture medium (Thermo Fisher, Waltham, MA) prior to transfection with dual- or triple-plasmid DNA. Transfection was completed using 1 mg/mL polyethylenimine (PEI) MAX (Polyscience, Warrington, PA) at a 2:1 ratio PEI:DNA, and 1 μ g of DNA per 1×10^6 cells was used for all transfections unless otherwise specified in the figure legend. 72 h post transfection, cells were lysed, and crude lysate samples were collected for productivity assessment following centrifugation or depth filtration to remove cellular debris.

VG productivity in number of vector genomes per cell (VG/cell) was determined by standard droplet digital PCR (ddPCR) method using primer and probe sets specific to the transgene payload of the vector. Briefly, vector samples were treated with RQ1 RNase-free DNaseI (Progema, Madison, WA) and proteinase K (Thermo Fisher, Waltham, MA) and diluted to the linear range of the assay. The reaction mixtures were assembled with the recommended ddPCR Supermix, TaqMan primers, and probes directed against a region of the transgene and template. Droplet generation is followed by amplification using a conventional thermal cycler. A Bio-Rad (Hercules, CA) QX200 droplet reader was used to scan the plate, and these data were analyzed with QuantaSoft software.

Capsid productivity was determined using a commercially available sandwich ELISA with an antibody specific for a conformational epitope on assembled AAV9 or AAV2 capsids (Progen, Wayne,

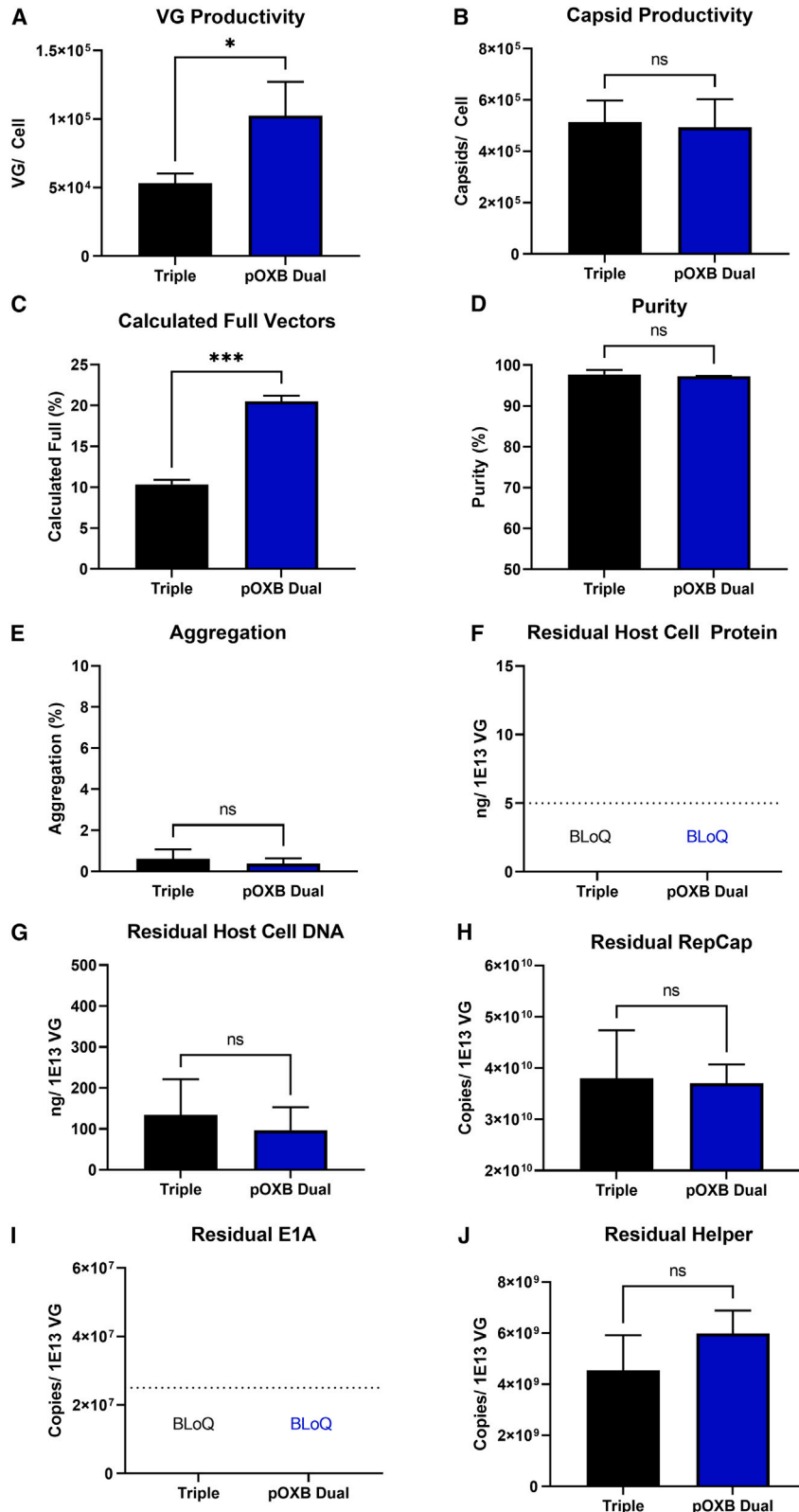


Figure 7. Productivity and product quality assessment of pOXB dual and triple plasmid produced drug substance

Genome D was produced at 50-L bioreactor scale using pOXB dual- (n = 2) and triple-plasmid (n = 3) transfection. Crude lysate samples were analyzed for (A) VG productivity, (B) capsid productivity, and (C) calculated full vectors, while purified vectors from these lots were analyzed for (D) purity, (E) aggregation, (F) residual host cell protein, (G) residual packaged host cell DNA, (H) residual packaged RepCap plasmid DNA, (I) residual packaged E1A DNA, and (J) residual packaged helper plasmid DNA. Data are displayed as mean ± SD. The dashed lines indicate the limit of detection for the assays where samples were determined to be below the limit of quantification (BLoQ). Statistical significance was determined using a Student's t test, *p < 0.05, ***p < 0.001; ns, not significant.

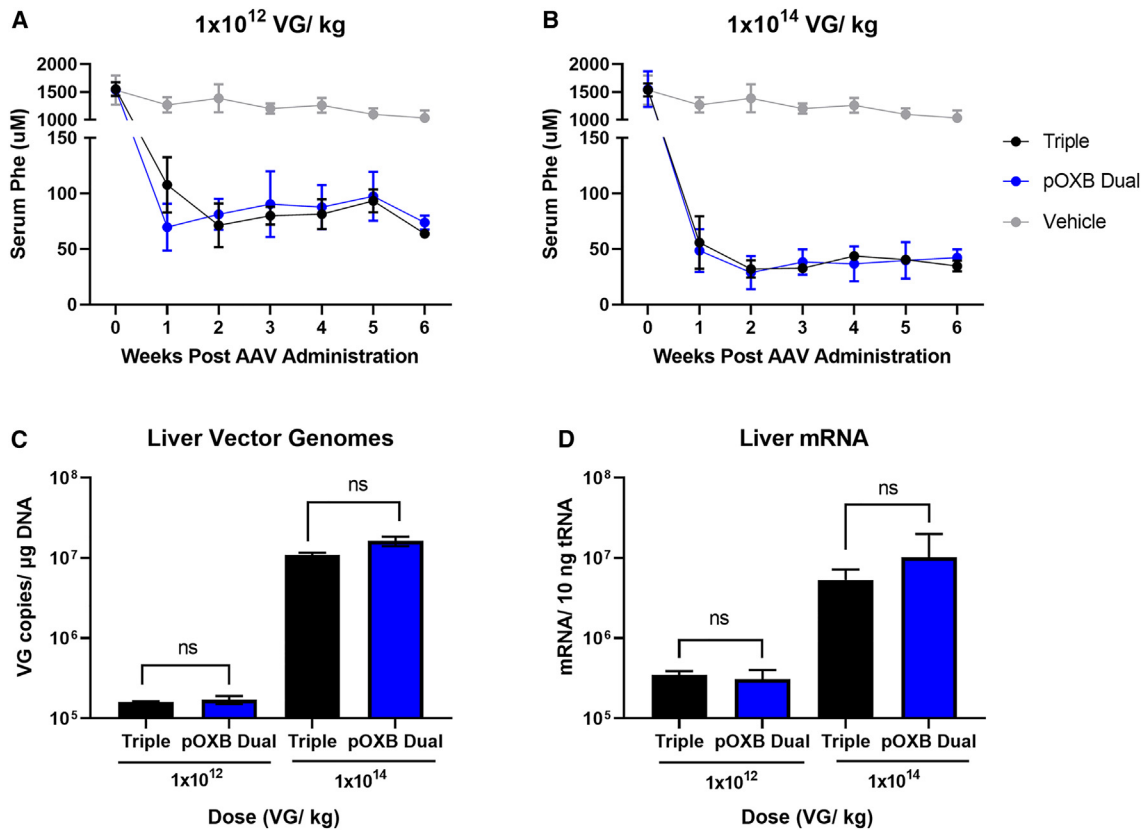


Figure 8. Comparison of *in vivo* bioactivity of pOXB dual and triple transfection vectors

BTBR Pah^{enu2} mice were systemically injected with (A) a low dose of 1×10^{12} VG/kg or (B) a high dose of 1×10^{14} VG/kg of vector produced by pOXB dual- or triple-plasmid transfection. A vehicle-only injection group was included as a negative control. Mice were monitored over 6 weeks including weekly serum Phe analysis. At endpoint, liver samples were collected to analyze (C) VGs and (D) mRNA expression. Statistical significance was determined using a Student's *t* test; ns, not significant.

PA). These data were normalized to the number of viable cells at the time of transfection. The percentage of full capsids was calculated by dividing the ddPCR VG titer by the capsid ELISA titer.

Vector quality assessment

Vectors were purified by affinity chromatography and further enriched for full capsids using anion exchange chromatography prior to vector quality assessments.

AUC was used to quantify empty capsids as well as capsids that contain full-length intact and partial rAAV genomes. Sedimentation velocity centrifugation was performed using the Optima AUC (Beckman Coulter, Brea, CA). Analysis of AAV samples by the SEDFIT c(S) model yields a distribution of sedimentation coefficients with each peak in the distribution representing an intact AAV genome or product residuals in the form of partial packaged genomes and empty capsids. Integration of the individual peaks yield the sedimentation coefficient (S) and the relative concentration of each species in the distribution.²¹ The linear relationship between S and the length (in nucleotides) of the packaged transgene can be used to predict the S value of a fully packaged AAV.

Capillary electrophoresis in the presence of sodium dodecyl sulfate (CE-SDS) was used to measure vector purity. Samples were denatured at 60°C and separated by increasing size and detected by absorbance at 220 nm using Beckman Coulter PA800 Plus (Brea, CA).

Size-exclusion chromatography by ultra-performance liquid chromatography (SEC-UPLC) was used to determine the amount of AAV aggregation present in the vector sample as determined by the sum of the area of all aggregate peaks and reported as a percentage relative to the total area, including vector monomers. Analysis was performed on an Agilent 1290 UHPLC system.

A commercially available ELISA kit was used to detect and quantitate residual levels of HEK293 host cell proteins in purified vector samples according to manufacturing instructions (Cygnus Technologies).

The concentration of residual host cell DNA in packaged vector was determined by quantitative PCR (qPCR)-based assay. Viral DNA was extracted using the QIAamp RNA Viral Mini Kit, and qPCR was performed using a primer/probe set directed to a repetitive element present in human DNA. The output of the assay was normalized by the VG titer.

ddPCR was used to quantify residual RepCap, E1a, and helper sequences in purified vectors. Purified samples were treated with proteinase K and diluted within the linear range of the ddPCR assay. Reactions were assembled and analyzed as described above using primer/probes sets specific to each target sequence. The output of the assay was normalized by the VG titer.

Flow cytometry

1 mL of culture was collected at approximately 72 h after transfection and processed using a BD Accuri C6 Plus flow cytometer equipped with an autosampler (BD Biosciences, San Jose, CA). At least 50,000 events were collected per sample with the fluidics rate set to slow (14 μ L/min) and one agitation/SIP clean cycle between samples. The acquired data were next analyzed in FlowJo software (v10.8; FlowJo, Ashland, OR) using standard gating strategy to select for single cells (based on SSC-A vs. FSC-A and FSC-H vs. FSC-A scatterplots) and to calculate the percentage of GFP-expressing cells (based on FITC-A histogram).

Western immunoblotting analysis

Lysate from cell pellets containing 3E6 cells was mixed with loading dye (VWR Radnor, PA) and denatured before being equally loaded onto a precast gel (Bio-Rad Hercules, CA) with a protein ladder (LI-COR BioSciences, Lincoln, NE). The gel was transferred onto a nitrocellulose membrane using the iBLOT transfer system (Thermo Fisher, Waltham, MA). A total protein stain (LI-COR BioSciences) was applied, and the membrane was imaged on the Odyssey CLx Imaging System (LI-COR BioSciences) for quantification purposes. The membrane was incubated in Odyssey PBS blocking buffer (LI-COR BioSciences) prior to incubation with primary antibody overnight at 4°C. B1 primary antibody (American Research Product, Waltham MA) was used to detect VP1, VP2, and VP3 expression at a 1:1,000 dilution, and anti-Rep (American Research Product, Waltham MA) was used at a 1:250 dilution in blocking buffer. After washing, the membrane was incubated in the secondary antibody, IRDye 680RD Goat anti-Mouse IgG Secondary Antibody (LI-COR biosciences), before being imaged on the Odyssey CLx. For quantification, the signal from each band was measured and normalized against the total protein stain signal for each lane.

Animals

All procedures were approved by the Institutional Animal Care and Use Committee at Homology Medicines. A colony of BTBR Pah^{enu2} was maintained in the animal facility at Homology Medicines under standard laboratory conditions, and animals were supplied with food and water *ad libitum*. 6- to 8-week-old male BTBR Pah^{enu2} mice were administered vector by retro-orbital injection following randomization based on baseline serum Phe concentrations. Serum was drawn weekly by submandibular bleed to monitor serum Phe concentrations as previously described.²² At endpoint, animals were euthanized and perfused with 1x PBS. Liver samples were harvested and snap frozen or stored in RNAlater for DNA and RNA extraction respectively.

Liver VG and mRNA quantification

Frozen liver tissue was homogenized using Precellys 24 tissue homogenizer, and genomic DNA was extracted using the QIAasympphony DSP DNA mini kit (Qiagen, Hilden, Germany). Total liver RNA was extracted from mouse livers using QIAgen RNeasy Mini Kit (Qiagen, Hilden, Germany) and reverse-transcribed into cDNA using the High-capacity cDNA Reverse Transcription Kit (Applied Biosystems, Waltham, MA). Liver VGs and mRNA were quantified by TaqMan qPCR against the GOI using a linearized plasmid standard containing the same GOI sequence as the vector.

Statistics

Statistical analysis was completed with GraphPad Prism software using one-way ANOVA or Student's t tests where applicable. All error bars represent the mean \pm standard deviation.

DATA AVAILABILITY

The authors confirm that the data supporting the findings of these studies are available within the article and its [supplemental information](#). Raw data were generated at Oxford Biomedica Solutions, and data supporting the findings of these studies are available from the corresponding author upon request.

SUPPLEMENTAL INFORMATION

Supplemental information can be found online at <https://doi.org/10.1016/j.omtm.2023.05.004>.

ACKNOWLEDGMENTS

The work described in this manuscript was funded by Homology Medicines, Inc., and Oxford Biomedica Solutions LLC. All authors were employed at Oxford Biomedica Solutions or Homology Medicines during their contributions to the manuscript. We wish to thank all those who contributed to the analytical data presented in this manuscript.

AUTHOR CONTRIBUTIONS

L.P.v.L., K.C.-G., K.S., M.S., I.I., N.A., J.Y., and T.K. designed the experiments. L.P.v.L., M.R., K.C.-G., S.O., D.G., T.P., E.W., K.S., D.G., M.S., B.B., J.G., I.I., G.Y., I.G., A.M., R.D., T.T., L.M., A.H., A.R., and J.L. executed experiments and analyzed data. L.P.v.L. drafted the manuscript with input from K.C.-G., D.G., J.M., J.Y., and T.K.

DECLARATION OF INTERESTS

All authors have received salary with employee stock options and/or restricted stock units during their employment at Oxford Biomedica Solutions LLC or Homology Medicines, Inc. L.P.v.L. and M.S. are inventors of patents associated with the pOXB dual-plasmid system.

REFERENCES

1. Matsushita, T., Elliger, S., Elliger, C., Podsakoff, G., Villarreal, L., Kurtzman, G.J., Iwaki, Y., and Colosi, P. (1998). Adeno-associated virus vectors can be efficiently produced without helper virus. *Gene Ther.* 5, 938–945.
2. Ayuso, E., Mingozzi, F., and Bosch, F. (2010). Production, purification and characterization of adeno-associated vectors. *Curr. Gene Ther.* 10, 423–436.

3. European Medicines Agency (2020). Assessment report: Zolgensma. https://www.ema.europa.eu/en/documents/assessment-report/zolgensma-epar-public-assessment-report_en.pdf.
4. U.S. Food and Drug Administration (2017). Summary basis for regulatory action: Luxturna. <https://www.fda.gov/media/110141/download>.
5. Grimm, D., Kern, A., Rittner, K., and Kleinschmidt, J.A. (1998). A novel tools for production and purification of recombinant adeno-associated virus vectors. *Hum. Gene Ther.* 9, 2745–2760.
6. Tang, Q., Keeler, A.M., Zhang, S., Su, Q., Lyu, Z., Cheng, Y., Gao, G., and Terence, T.F. (2020). Two-plasmid packaging system for recombinant adeno-associated virus. *Biores Open Access* 9, 219–228.
7. Smith, L.J., Ul-Hasan, T., Carvaines, S.K., Van Vliet, K., Yang, E., Wong, K.K., Jr., Agbandje-McKenna, M., and Chatterjee, S. (2014). Gene transfer properties and structural modeling of human stem cell-derived AAV. *Mol. Ther.* 22, 1625–1634.
8. Ellsworth, J.L., Gingras, J., Smith, L.J., Rubin, H., Seabrook, T.A., Patel, K., Zapata, N., Olivieri, K., O’Callaghan, M., Chlipala, E., et al. (2019). Clade F AAVHSCs cross the blood brain barrier and transduce the central nervous system in addition to peripheral tissues following intravenous administration in nonhuman primates. *PLoS One* 14, e0225582.
9. Grimm, D., Kay, M.A., and Kleinschmidt, J.A. (2003). Helper virus-free, optically controllable, and two-plasmid-based production of adeno-associated virus vectors of serotypes 1 to 6. *Mol. Ther.* 7, 839–850.
10. Meier, A.F., Fraefel, C., and Seyffert, M. (2020). The interplay between adeno-associated virus and its helper viruses. *Viruses* 12, 662.
11. Ward, P., Clément, N., and Linden, R.M. (2007). Cis effects in adeno-associated virus type 2 replication. *J. Virol.* 81, 9976–9989.
12. Nonnenmacher, M., van Bakel, H., Hajjar, R.J., and Weber, T. (2015). High capsid–genome correlation facilitates creation of AAV libraries for directed evolution. *Mol. Ther.* 23, 675–682.
13. Werle, A.K., Powers, T.W., Zobel, J.F., Wappelhorst, C.N., Jarrold, M.F., Lykтей, N.A., Sloan, C.D.K., Wolf, A.J., Adams-Hall, S., Baldus, P., and Runnels, H.A. (2021). Comparison of analytical techniques to quantitate the capsid content of adeno-associated viral vectors. *Mol. Ther. Methods Clin. Dev.* 23, 254–262.
14. Shedlovsky, A., McDonald, J.D., Symula, D., and Dove, W.F. (1993). Mouse models of human phenylketonuria. *Genetics* 134, 1205–1210.
15. Merten, O.W., Gény-Fiamma, C., and Douar, A.M. (2005). Current issues in adeno-associated viral vector production. *Gene Ther.* 12, S51–S61.
16. Yin, J. (2022). Achieving rAAV Bioreactor Titer Of >1E15 vg/L With Novel Plasmid Transient Transfection Platform (Bioprocess Online). <https://www.bioprocessonline.com/doc/achieving-raav-bioreactor-titer-of-e-vg-l-with-novel-plasmid-transient-transfection-platform-0001>.
17. Xie, J., Mao, Q., Tai, P.W.L., He, R., Ai, J., Su, Q., Zhu, Y., Ma, H., Li, J., Gong, S., et al. (2017). Short DNA hairpins compromise recombinant adeno-associated virus genome homogeneity. *Mol. Ther.* 25, 1363–1374.
18. Dong, B., Nakai, H., and Xiao, W. (2010). Characterization of genome integrity for oversized recombinant AAV vector. *Mol. Ther.* 18, 87–92.
19. Mullard, A. (2021). Gene therapy community grapples with toxicity issues, as pipeline matures. *Nat. Rev. Drug Discov.* 20, 804–805.
20. U.S. Food and Drug Administration Center for Biologics Evaluation and Research (2021). 70th cellular, tissue and gene therapies advisory committee meeting transcript. <https://www.fda.gov/media/154397/download>.
21. Burnham, B., Nass, S., Kong, E., Mattingly, M., Woodcock, D., Song, A., Wadsworth, S., Cheng, S.H., Scaria, A., and O’Riordan, C.R. (2015). Analytical ultracentrifugation as an approach to characterize recombinant adeno-associated viral vectors. *Hum. Gene Ther. Methods* 26, 228–242.
22. Ahmed, S.S., Rubin, H., Wang, M., Faulkner, D., Sengooba, A., Dollive, S.N., Avila, N., Ellsworth, J.L., Lamppu, D., Lobikin, M., et al. (2020). Sustained correction of a murine model of phenylketonuria following a single intravenous administration of AAVHSC15-PAH. *Mol. Ther. Methods Clin. Dev.* 17, 568–580.

Supplemental information

A novel dual-plasmid platform provides scalable transfection yielding improved productivity and packaging across multiple AAV serotypes and genomes

Laura P. van Lieshout, Miranda Rubin, Katrina Costa-Grant, Stacy Ota, Diane Golebiowski, Troy Panico, Eli Wiberg, Klaudia Szymczak, Richard Gilmore, Marissa Stanvick, Brenda Burnham, Jeff Gagnon, Ifeyinwa Iwuchukwu, Guang Yang, Iraj Ghazi, Alex Meola, Ryan Dickerson, Thomas Thiers, Luke Mustich, April Hayes, Israel Rivas, Jason Lotterhand, Nancy Avila, James McGivney, Jin Yin, and Tim Kelly

Supplemental Material

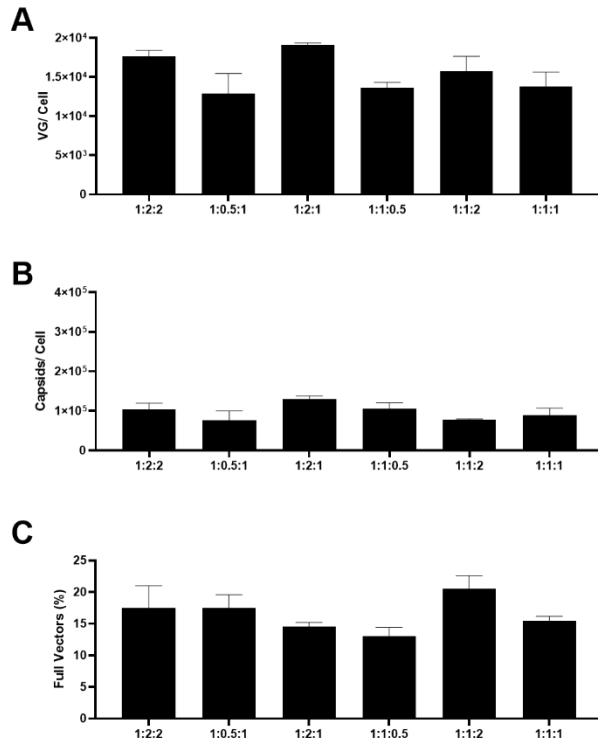


Figure S1: Productivity Assessment of Triple Transfection. Shake flasks were transfected with triple plasmids at molar ratios of 1:2:2, 1:0.5:1, 1:2:1, 1:1:0.5, 1:1:2 and 1:1:1 GOI-ITR: RepCap: Helper. Crude lysate samples were quantified for (A) VG production (B) capsid production and (C) calculated full vectors. All conditions were completed in duplicate, and the data is displayed as mean \pm SD.

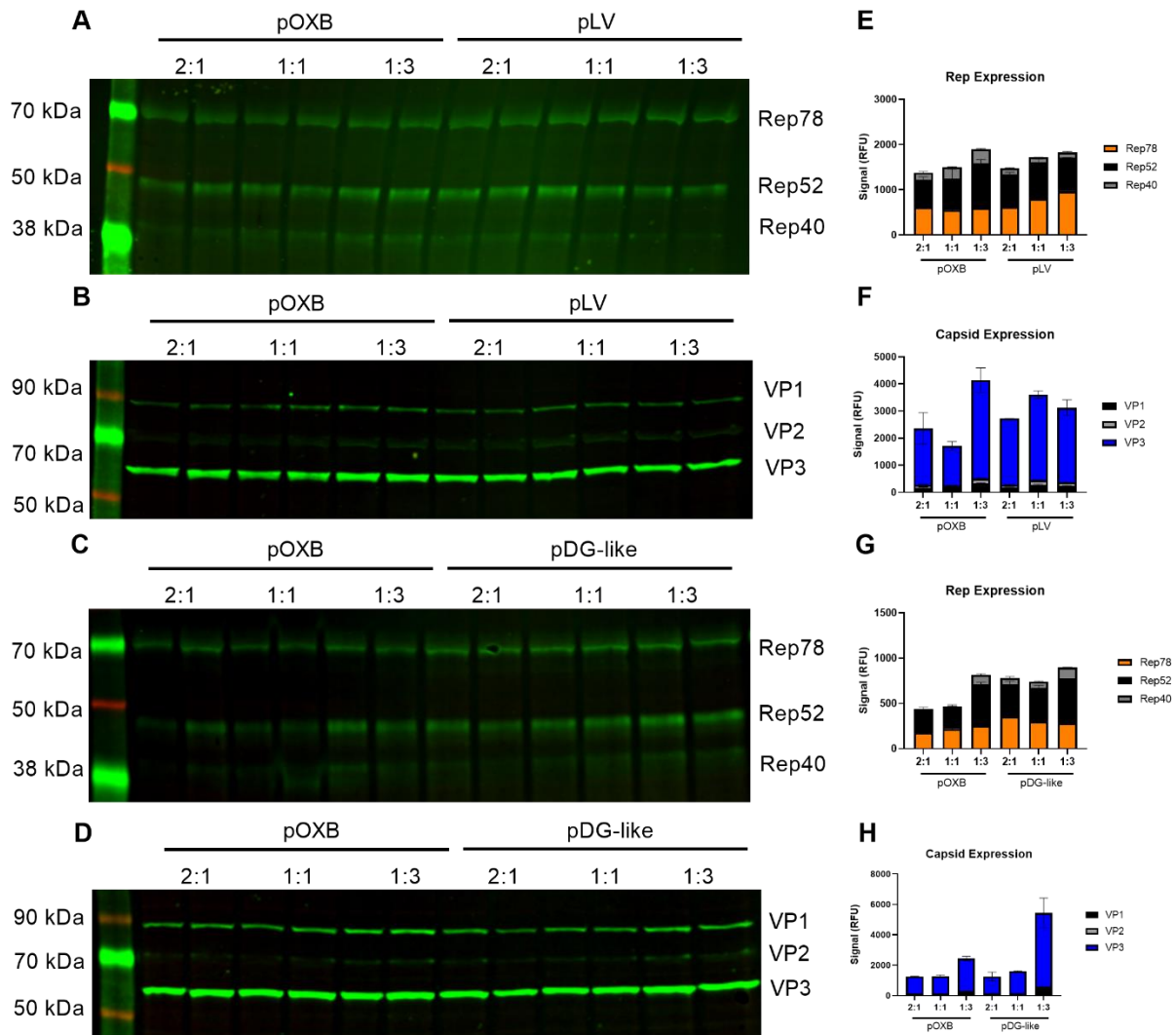


Figure S2: Expression of Rep and Cap from pOXB, pLV and pDG-like Plasmid Designs.

Shake flasks were transfected with GOI-ITR genome G using the pOXB, pLV or pDG-like dual plasmid systems. Western blot analysis was performed on crude lysates to detect (A, C) Rep and (B, D) Cap expression. Quantification of (E, G) Rep and (F, H) Cap expression from the western blot is shown. All conditions were completed in duplicate, and the data is displayed as mean \pm SD.

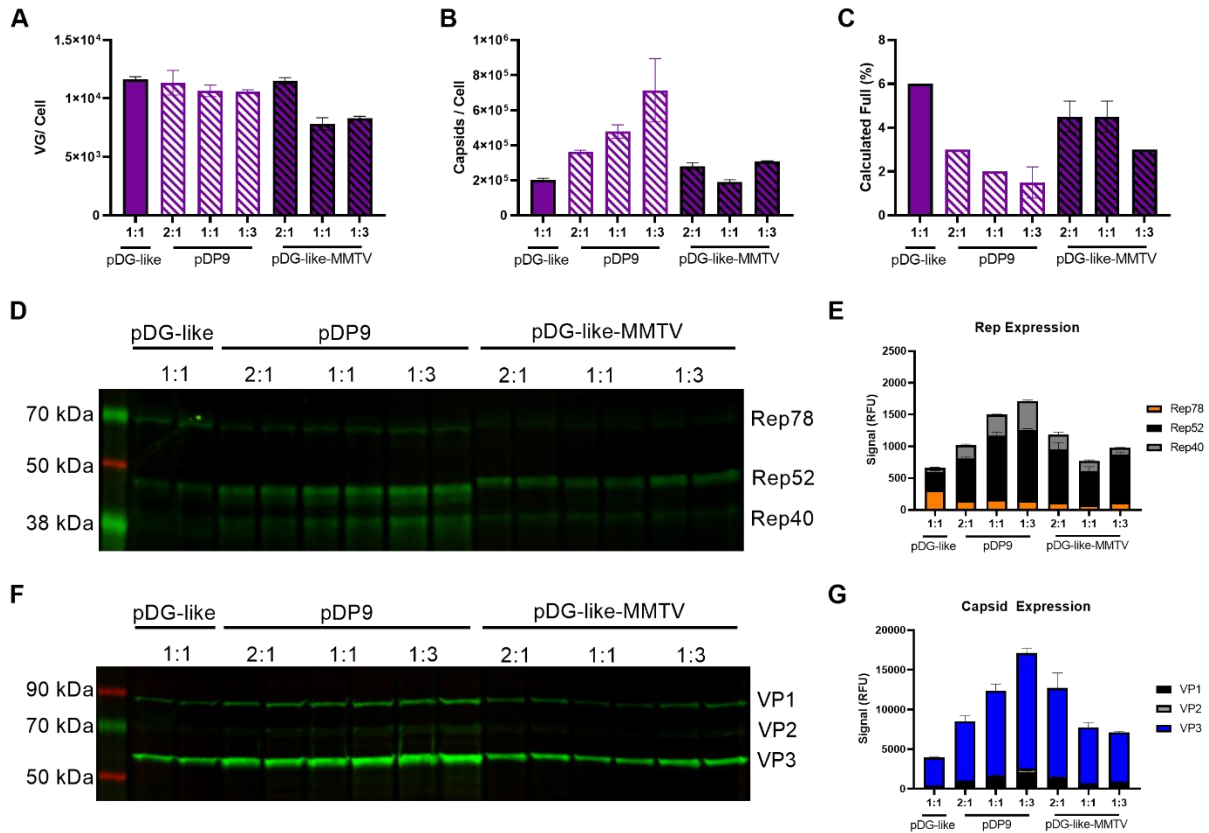


Figure S3: Productivity Assessment of pDG-like, pDG-like-MMTV and pDP9. Shake flasks were transfected with GOI-ITR genome G and pDG-like, pDG-like-MMTV or pDP9 RepCap+Helper plasmids. Molar plasmid ratios are displayed as GOI-ITR: RepCap+Helper. pDP9 contains the AAV9 capsid sequence. Crude lysate samples were quantified for (A) VG productivity (B) capsid productivity and (C) the percentage of calculated full vectors. Western blot analysis was performed on crude lysates to detect (D) Rep and (F) Cap expression. Quantification of (E) Rep and (G) Cap expression from the western blot is shown. All conditions were completed in duplicate, and the data is displayed as mean ± SD.

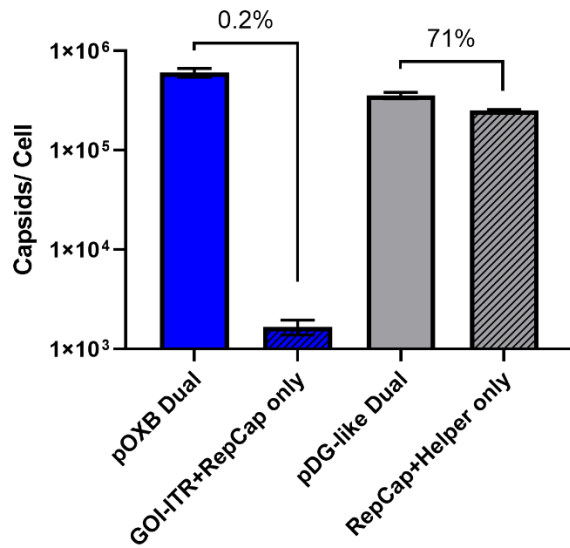


Figure S4: Background Capsid Expression Following Transfection of Only the RepCap Containing Plasmid for pDG-like and pOXB Dual Systems. pOXB and pDG-like dual plasmids were transfected using genome D in shake flasks at a 1:1 molar ratio. Transfections containing only the RepCap-bearing plasmid were completed using the same quantity of plasmid used in the dual system transfections: 44.1 $\mu\text{g}/1\text{E}6$ cells for pOXB and 55.9 $\mu\text{g}/1\text{E}6$ cells for pDG-like. All conditions were completed in duplicate, and the data are displayed on the graph as mean \pm SD.

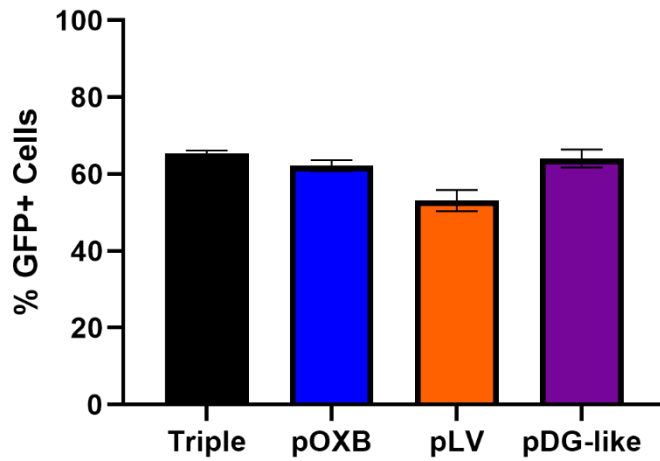


Figure S5: Proportion of Cells Expressing GFP Post-transfection with Each Plasmid

System. Shake flasks were transfected with pOXB, pDG-like, pLV dual or triple plasmids using GOI-ITR genome G sequence at a 1:1 or 1:1:1 molar ratio with the first plasmid containing the GOI-ITR sequence. Crude lysate samples were quantified for percentage of cells that were GFP positive 72 hours post transfection. All conditions were completed in duplicate, and the data is displayed as mean \pm SD.

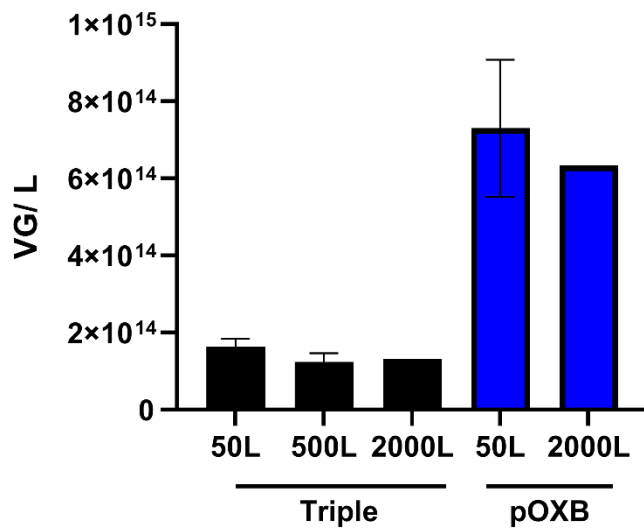


Figure S6: Consistent Vector Genome Productivity Across 50L to 2000L Bioreactor Scale. Genome D was produced by triple and pOXB dual transfection using a platform upstream process at multiple scales. Average crude lysate VG productivity is displayed as mean \pm SD, 50L (n=12), 500L (n=4) and 2000L (n=1) for triple and 50L (n=4) and 2000L (n=1) for pOXB dual.

Table S1: Plasmid Sizes

ITR-GOI Containing Plasmids			
	Triple	pOXB	pLV
Genome A	6,619 bp	10,893 bp	15,924 bp
Genome B	7,113 bp	11,505 bp	n/a
Genome C	5,182 bp	9,574 bp	n/a
Genome D	5,041 bp	9,433 bp	n/a
Genome E	6,847 bp	11,140 bp	n/a
Genome F	6,329 bp	11,209 bp	n/a
Genome G	4,822 bp	9,214 bp	14,165 bp
Non-ITR-GOI Containing Plasmids			
RepCap	7,043 bp		
Helper	11,990 bp		
pDG-like	16,345 bp		
pDG-MMTV	16,963 bp		

n/a- not applicable, bp- base pairs

Table S2: Description of rAAV Genomes Evaluated

Genome	Promoter	Transgene	Size (nt)	Genome Design (SS or SC)
Genome A	n/a	I	3,939	SS
Genome B	A	I	4,452	SS
Genome C	B	II	2,521	SS
Genome D	A	I	4,606	SC
Genome E	A	I	4,186	SS
Genome F	C	III	4,483	SS
Genome G	D	IV	2,162	SS

nt- nucleotides, SS- single stranded genome, SC- self-complementary genome